Simple and Accurate Calibration of the Flory-Huggins Interaction Parameter

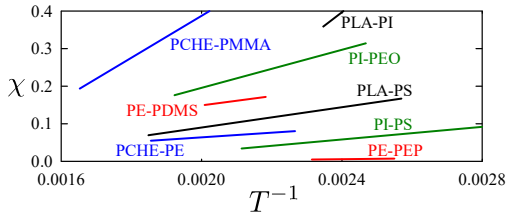
J. D. Willis,[†] T. M. Beardsley,[†] and M. W. Matsen[*,†,‡,¶]

[†]*Department of Physics & Astronomy, University of Waterloo, Waterloo, Ontario, Canada*

[‡]*Department of Chemical Engineering, University of Waterloo, Waterloo, Ontario, Canada*

[¶]*Waterloo Institute for Nanotechnology, University of Waterloo, Waterloo, Ontario, Canada N2L 3G1*

E-mail: mwmatsen@uwaterloo.ca



Abstract

This paper improves upon a standard method of determining the Flory-Huggins χ parameter, whereby experimental order-disorder transitions (ODTs) of symmetric diblock polymer melts are fit to the mean-field prediction, $(\chi N)_{\mathrm{ODT}} = 10.495$. The improvement is achieved by switching to an accurate prediction of $(\chi N)_{\mathrm{ODT}}$ from Morse and coworkers, supplemented with corrections for the small degrees of polydispersity and compositional asymmetry that inevitably exist in real diblock polymers. The first correction is evaluated by simulating polydisperse diblocks over a wide range of invariant polymerization indices, and the second correction is extracted from analogous simulations for compositionally asymmetric diblocks by Ghasimakbari and Morse. The resulting calibration method is then demonstrated on 19 different chemical pairs, using previously published experimental data. It provides a considerable increase in accuracy, but yet is nearly as simple to apply as the original version.

Introduction

The behavior of block polymer melts is understood to be universal,[1] which implies that all systems can be represented by the standard Gaussian-chain model (GCM)[2] in the limit of high molecular weight. The GCM is a minimal model that treats a melt as an incompressible system of elastic threads interacting by pairwise contact forces. Its mean-field behavior for monodisperse AB diblock polymers, as predicted by self-consistent field theory (SCFT),[2–6] is controlled by just three quantities: the composition f, the ratio of segment lengths a_A/a_B, and the product χN, where N is the number of segments of volume ρ_0^{-1} per molecule and χ is the Flory-Huggins interaction parameter. Fluctuation corrections to the mean-field behavior are then controlled by one additional parameter: the invariant polymerization index $\bar{N} = a^6\rho_0^2 N$, where $a = [fa_A^2 + (1-f)a_B^2]^{1/2}$ is the average segment length.[7] To exploit this universality, one needs to map the parameters of a given system onto those of the standard GCM. The mapping of molecular compositions (e.g., f) is trivial given their

straightforward definition in terms of volume fraction. Segment lengths are also clearly defined by the fact that the radius of gyration of a linear polymer in an athermal melt reduces to $R_g = a(N/6)^{1/2}$ in the limit of large N. The only nontrivial part of the mapping is determining the χ parameter.

The determination of χ has been a longstanding problem to which numerous strategies have been applied.[8–22] Unfortunately, the different methods generally result in different values of χ,[8–13] leading many to conclude that χ depends on architecture, composition, molecular weight, polydispersity, or basically all the details of the system. Others question whether or not there even exists a consistent definition for χ. The problem stems from the way χ is determined, which always involves measuring some quantity by experiment (or simulation) and then fitting to a prediction of the standard GCM. For χ to be accurate, not only does the measurement need to be accurate but so does the prediction. In most cases, the prediction is based on mean-field theory, which, in effect, buries fluctuation corrections into χ. Thus, it should be of no surprise that the χ values derived from different quantities are themselves different, since the quantities possess distinct fluctuation corrections. Furthermore, fluctuation effects depend on all the parameters of the system, and thus the resulting χ will also depend on all the parameters.

Morse and coworkers[23] have made great progress in remedying this shortcoming by instead fitting the peak of the disordered-state structure function, $S(q^*)$, of symmetric diblocks to renormalized one-loop (ROL) predictions,[24,25] arguably the most accurate calculation available. The improvement in χ is evident from the fact that it nicely reveals the universality of block polymer behavior among different systems. Glaser et al.[26] demonstrated this by comparing the order-disorder transition (ODT) of symmetric diblock polymer melts from five distinct models. When expressed in terms of the calibrated parameters, the ODTs from all five models collapsed onto a universal curve,

$$(\chi N)^{\rm ideal}_{\rm ODT} = 10.495 + 41.0\bar{N}^{-1/3} + 123.0\bar{N}^{-0.56} \qquad (1)$$

The equivalence between models has since been illustrated for a number of other quantities of symmetric diblocks.[27] More recently, the universality has been confirmed for asymmetric diblock polymer melts.[28,29]

Gillard et al.[30] have also applied the Morse calibration to an experimental system, specifically polylactide-polyisoprene (PLA-PI) diblock polymer melts. Using the calibration, they compared the experimental ODT, its latent heat, and the peak position of $S(q)$ to simulations. The agreement was reasonable, but not particularly impressive. They suggested a number of potential explanations, including the fact that the Morse calibration assumes monodisperse molecules, whereas the experiments involved a modest degree of polydispersity, $Đ = 1.10$. Indeed, when Beardsley and Matsen[31] later accounted for the polydispersity, the discrepancies disappeared.

Although the Morse calibration is easily applied to simulation models, the same is not true of experimental systems because it requires the absolute scattering intensity. Furthermore, as of yet, there are no ROL predictions of $S(q)$ for polydisperse melts. Beardsley and Matsen dealt with this by simulating $S(q)$ for polydisperse melts, using a model that had been previously calibrated against ROL predictions for monodisperse melts.

One of the common methods[11,32–39] of calibrating χ has been to fit the ODTs of symmetric diblock polymers of varying molecular weights, M_n, to the mean-field prediction, $(\chi N)_{\mathrm{ODT}} = 10.495$. The merits of this method are that the experimental T_{ODT} can be measured accurately and it has a strong dependence on χ, but the method suffers from the fact that the mean-field prediction is seriously inaccurate, particularly for short molecules. To improve the accuracy, a few studies[11,40] have fit the ODTs to the Fredrickson-Helfand prediction, $(\chi N)_{\mathrm{ODT}} = 10.495 + 41.0\bar{N}^{-1/3}$, and for even better accuracy, some studies[13,41,42] are now fitting to eq 1. However, this still assumes that the diblock polymers are monodisperse and perfectly symmetric.

In order to account for deviations from this ideal, we write

$$(\chi N)_{\mathrm{ODT}} = \Gamma \times (\chi N)^{\mathrm{ideal}}_{\mathrm{ODT}} \tag{2}$$

where the correction factor, Γ, depends on f, Đ, a_A/a_B, and $\bar{N}$. Provided that the deviations from Đ = 1 and $f = \frac{1}{2}$ are small, the correction factor can be approximated by a truncated Taylor series,

$$\Gamma \approx 1 + \gamma_1(Đ - 1) + \gamma_2(f - \tfrac{1}{2})^2 \tag{3}$$

For now, we continue to assume $a_A = a_B$, and therefore the linear term, $f - \frac{1}{2}$, vanishes due to symmetry. The coefficients, γ_1 and γ_2, will both depend on the remaining parameter, $\bar{N}$. We determine the dependence for γ_1 by performing simulations of polydisperse diblocks and for γ_2 by referring to previous simulations of compositionally asymmetric diblocks by Ghasimakbari and Morse.[29] Equations 2 and 3 are then used to obtain more accurate predictions for χ by reanalyzing previous fits to $(\chi N)_{\mathrm{ODT}} = 10.495$, which is possible thanks to the common experimental practise of reporting Đ and f values.

Lattice Model Simulations

To determine the polydispersity correction, γ_1, over a wide range of $\bar{N}$ values, we simulate polydisperse melts using a multiple-occupancy lattice model.[43] In particular, the polymerizations of the A and B blocks, N_{A} and N_{B}, are each approximated by the same continuous Schulz-Zimm distribution,[44,45]

$$p(N_\gamma) = \frac{k^k N_\gamma^{k-1}}{(N_\gamma)_n^k \Gamma(k)} \exp\left(-\frac{kN_\gamma}{(N_\gamma)_n}\right) \tag{4}$$

where the polydispersity index and number-average polymerization of the γ block are $Đ_\gamma = (k+1)/k$ and $(N_\gamma)_n$, respectively. Reference 46 details our procedure for creating a discrete distribution from eq 4. The diblocks are then formed by randomly pairing A and B blocks,

such that their total polydispersity index and number-average polymerization are given by $Đ = Đ_\gamma/2$ and $N = 2(N_\gamma)_n$, respectively.

The melt is modeled by placing the diblock polymers on an fcc lattice, with their monomers constrained to the lattice sites and bonded monomers occupying nearest-neighbor sites. The coordinates of each site i assume the form $\mathbf{r}_i = d(h, k, l)$, where h, k and l take on integers between 1 and L such that their sum, $h + k + l$, is even. Thus, the lattice has a total of $M = L^3/2$ sites and a nearest-neighbor distance of $b = \sqrt{2}d$. The application of periodic boundary conditions requires L to be even. The ability to cover a wide range of $\bar{N}$ values is achieved by controling the occupancy of the lattice sites, Z. To allow room for the polymers to move, 20% of the sites contain a single vacancy (i.e., a reduced monomer occupancy of $Z - 1$), which leads to an average monomer density of

$$\rho_0 \equiv nN/V = (Z - 0.2)\sqrt{2}/b^3 \tag{5}$$

where n is the total number of diblocks and $V = (Ld)^3 = Mb^3/\sqrt{2}$ is the volume of the system.

The Hamiltonian of the melt is assigned the simple form

$$\frac{H}{k_B T} = \alpha n_{AB} \tag{6}$$

involving a dimensionless interaction parameter, α, times the total number of A-B contacts,

$$n_{AB} = \sum_{i,j=1}^{M} \Delta_{ij} n_{A,i} n_{B,j} \tag{7}$$

where $n_{\gamma,i}$ is the number of γ-type monomers at site i. For computational efficiency, it is best to set Δ_{ij} equal to the Kronecker delta function, δ_{ij}, so that monomers only interact with others on the same lattice site.[43] Of course, this requires there to be multiple monomers per site. Therefore, for $Z \leq 2$, we increase the range of the interactions to include nearest

neighbors by setting $\Delta_{ij} = 1$ if $|\mathbf{r}_i - \mathbf{r}_j| \leq b$ and 0 otherwise.

The equilibrium behavior of this model is simulated in the canonical ensemble using the Metropolis Monte Carlo algorithm, where the Monte Carlo steps (MCS) randomly select among four different trial moves. The first is a slithering snake (or reptation) move. It is performed by randomly choosing one of the chain ends, and moving it to a randomly chosen nearest-neighbor site. The remaining monomers of the chain are then shifted one site along its contour. The move is immediately rejected if it causes a violation in the allowed number of monomers at any site, and otherwise its acceptance is determined by the Metropolis criterion. The second is a crankshaft move, where one of the non-end monomers is selected at random and moved while keeping its two bonded neighbors fixed. If the initial site already has a vacancy or there are no potential sites with a vacancy, then the move is rejected. Otherwise, one of the potential sites is selected at random and the Metropolis criterion is applied. The third is a double-bridging move that swaps A-type (or B-type) tails of equal length between two polymers. This move is performed by selecting a random site and looking for pairs of A (or B) monomers equal distance from the A (or B) ends of their respective chains. If no pairs of identical homopolymer tails exist, then the move is rejected. Otherwise, we choose the longest pair of tails and swap them between the two molecules. The last move is a chain reversal, where one of the diblock polymers is selected at random, and a complete head-to-tail flip is attempted.

Morse Calibration of the Model

The relationship between the interaction parameter of the lattice model, α, and the Flory-Huggins interaction parameter of the GCM, χ, is determined for $Z = 1$, 2, 3, and 5 following the Morse calibration procedure detailed in ref 43. The procedure starts by simulating monodisperse athermal melts (i.e., $Đ = 1$ and $\alpha = 0$) for a series of polymerizations, N. The

segment length is first obtained by fitting the radius of gyration to[47]

$$\frac{6R_g^2}{a^2N} = 1 - \frac{1.42}{a^3\rho_0 N^{1/2}} + \frac{\gamma}{N} \tag{8}$$

where a and γ serve as fitting parameters. The resulting segment lengths, a, are listed in Table 1, and the quality of the fits is illustrated in Figure 1. Once a is known, the invariant polymerization index can be evaluated using $\bar{N} = a^6\rho_0^2 N$.

Table 1: Calibration of the lattice model for different lattice site occupancies, Z.

Z	a/b	$\bar{N}/N$	z_∞	c_2	c_3
1	1.233	4.51	4.90	33.6	-74
2	1.113	12.4	16.1	208	-63
3	1.075	24.2	1.48	0.68	-0.17
5	1.045	59.9	3.34	4.15	-8.5

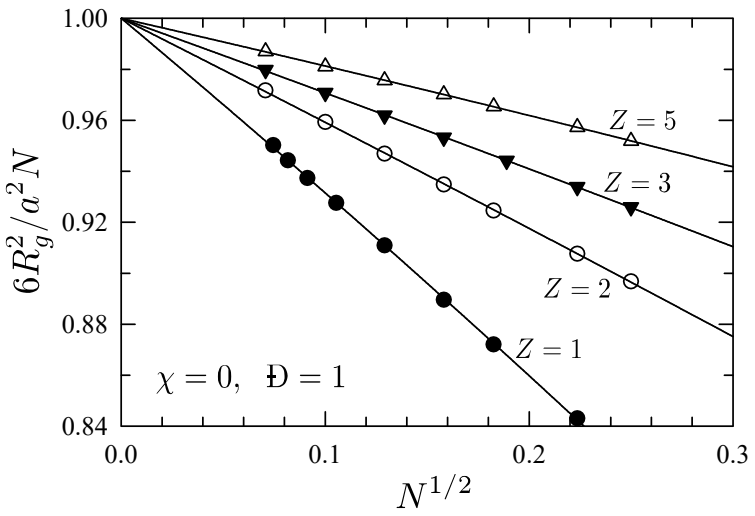


Figure 1: Radius of gyration squared, R_g^2, in an athermal melt plotted in terms of polymerization, N, for different lattice site occupancies, Z. Simulation results are denoted by symbols and fits to eq 8 are shown with solid curves.

For weak segregations, the Flory-Huggins parameter can be approximated by $\chi \approx z_\infty \alpha$, where $z_\infty = \lim_{N\to\infty} z(N)$ is the long-chain limit of the average number of intermolecular contacts per monomer, $z(N)$, in an athermal melt. Therefore, statistics for $z(N)$ are collected

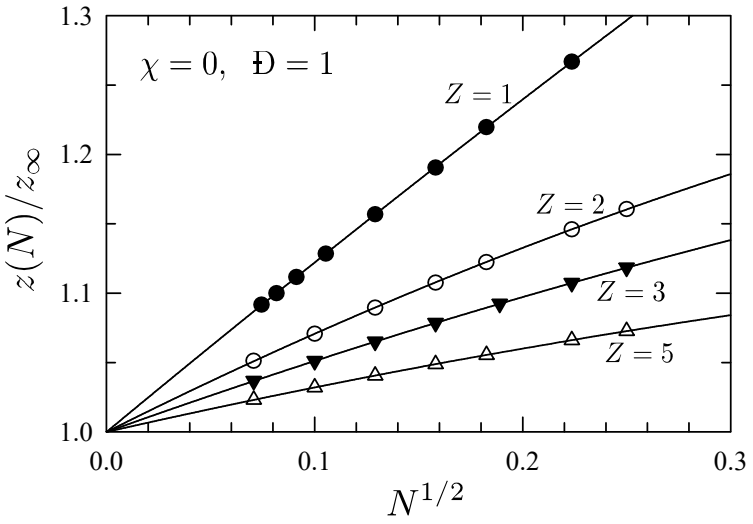


Figure 2: Number of intermolecular contacts per monomer, $z(N)$, in an athermal melt plotted in terms of polymerization, N, for different lattice site occupancies, Z. Simulation results are denoted by symbols and fits to eq 9 are shown with solid curves.

at the same time as those for R_g. The results for different polymerizations, N, are fit to[47]

$$\frac{z(N)}{z_\infty} = 1 + \frac{(6/\pi)^{3/2}}{a^3\rho_0 N^{1/2}} + \frac{\delta}{N} \tag{9}$$

where z_∞ and δ are the fitting parameters. The values of z_∞ are given in Table 1, and the quality of the fits is shown in Figure 2. Note that the non-monotonic behavior with respect to Z results because nearest-neighbor interactions are included for $Z \leq 2$.

To calculate corrections to the linear χ, the structure function of symmetric monodisperse diblocks, $S(q)$, is evaluated over the entire disordered phase for several different values of N. The peak of the structure function, $S(q^*)$, is then fit to renormalized one-loop (ROL) predictions assuming the nonlinear relationship

$$\chi(\alpha) = z_\infty\alpha + c_2\alpha^2 + c_3\alpha^3 \tag{10}$$

The coefficients of the fits, c_2 and c_3, are listed in Table 1, and the quality of the fits is demonstrated in Figure 3. Again, non-monotonic behavior with respect to Z occurs because of the change in the range of the interactions.

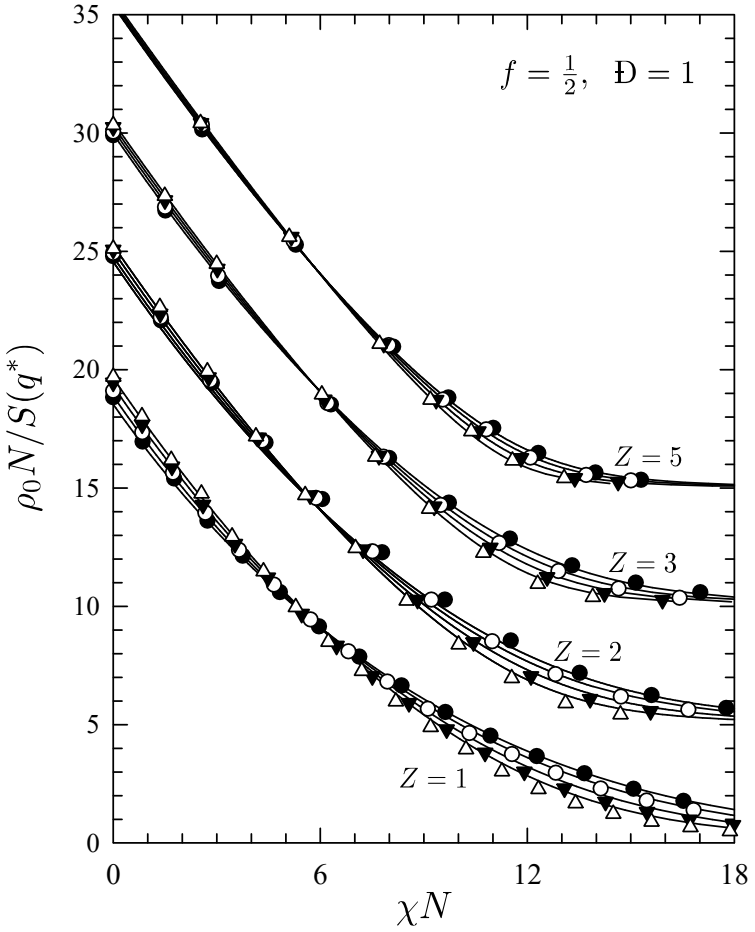


Figure 3: Inverse of the structure function peak, $S^{-1}(q^*)$, for symmetric monodisperse diblock melts plotted in terms of segregation, χN. Simulation results for $N = 30$, 40, 50, and 60 are denoted by solid circles, open circles, closed triangles, and open triangles, respectively, and fits to ROL are shown with solid curves. For clarity, the results for $Z = 2$, 3, and 5 are shifted upwards by 5, 10, and 15 units, respectively.

Symmetric Monodisperse Diblocks

Having calibrated the lattice model, we now illustrate that it adheres to the universality hypothesis, by comparing the ODT for monodisperse diblock polymers of $N = 50$ to eq 1. This is done by simulating multiple replicas of the system at a series of α values spanning the expected ODT, all initialized with disordered configurations. Based on SCFT predictions, the cubic simulation boxes are selected to be approximately three lamellar periods in size, which is sufficiently large to suppress finite-size effects.[48,49] The replicas are then run in parallel, each following the usual MC algorithm for approximately 10^6 MCS per monomer. The ODT is identified by evaluating the average number of A-B contacts, $\langle n_{\mathrm{AB}} \rangle$, over the last 10^4 MCS per monomer. Past studies[26,48] have demonstrated that $\langle n_{\mathrm{AB}} \rangle$ changes abruptly once the lamellar phase spontaneously forms.

During the simulations, highly metastable defects often nucleate impeding the formation of a well-ordered morphology, particularly when α is large. To help remedy this problem, we implement parallel tempering, whereby a swap between a random pair of replicas at neighboring α values is attempted every 10^3 MCS per monomer (see ref 48 for details). In this way, defect structures are shifted to lower segregation, which allows them to anneal out more easily. By the end of our simulations, all the ordered replicas exhibited defect-free lamellae. Even with parallel tempering, the metastability of the disordered phase may cause an overestimation of $(\chi N)_{\mathrm{ODT}}$. Therefore, we run a second set of parallel-tempering simulations, starting from ordered lamellar configurations obtained from the first runs. The second runs will tend to underestimate $(\chi N)_{\mathrm{ODT}}$, thus allowing us to bracket the true equilibrium ODT as shown in Figure 4.

Figure 5 compares the resulting ODTs to the universal prediction, eq 1. The error bars denote the widths of the metastability intervals, where the disordered and ordered runs remain in their initial phase over the duration of the simulation. The agreement in Figure 5 confirms that the model is well calibrated and that $N = 50$ is adequate to obtain universal behavior. The inset compares the period, D, of the lamellar phase at the ODT with the

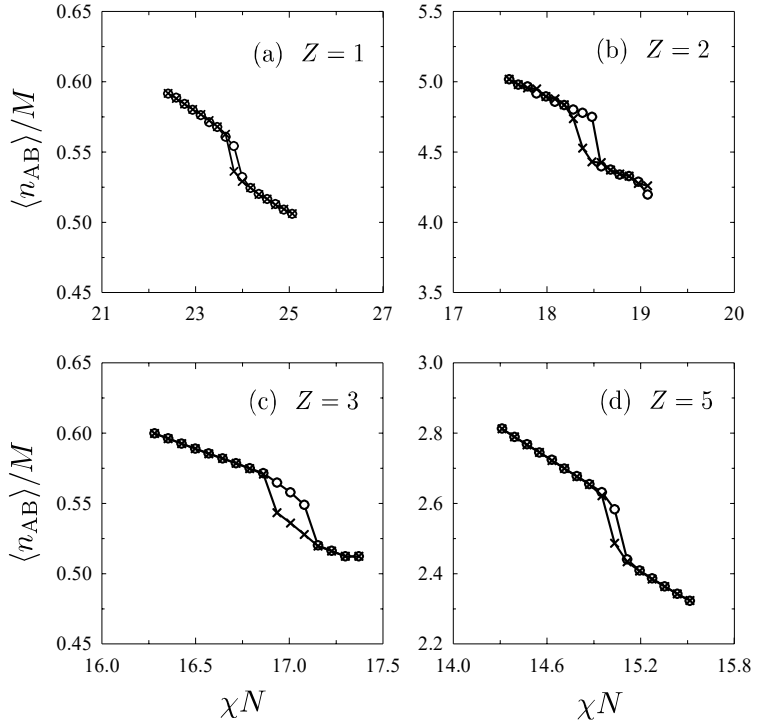


Figure 4: Average number of A-B contacts, $\langle n_{AB}\rangle$, for symmetric monodisperse diblock polymers of $N = 50$, obtained from parallel-tempering simulations with different lattice site occupancies, Z. Circles and crosses denote simulations initialized with disordered and ordered configurations, respectively.

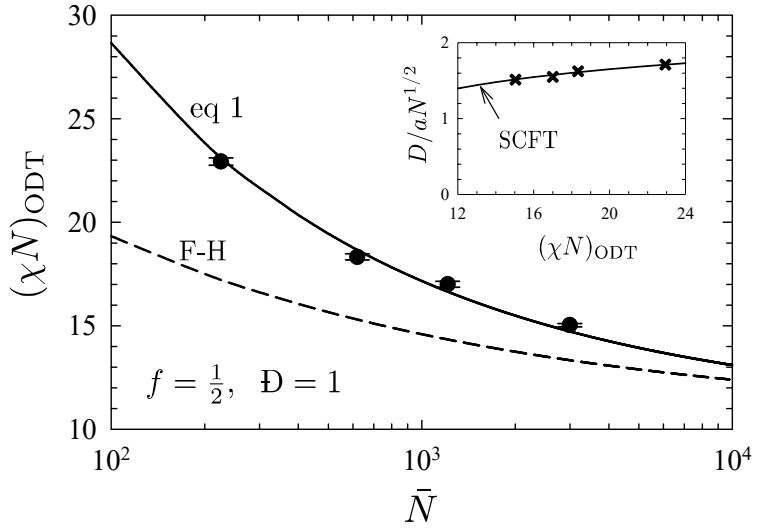


Figure 5: ODTs for symmetric monodisperse diblock polymers obtained from Figure 4. The solid curve denotes the universal prediction in eq 1,[26] and the dashed curve shows the Fredrickson-Helfand prediction.[7] The inset compares the lamellar periods, D, with the SCFT prediction.[3]

SCFT prediction[3] for the same value of χN. The agreement is consistent with previous findings that SCFT provides an accurate treatment of ordered phases.[27,29]

Corrections for Polydispersity and Compositional Asymmetry

Now that the behavior of monodisperse diblocks has been established, the parallel-tempering simulations are repeated for polydisperse melts with small indices, Đ = 1.05 and 1.10, typical of experiments used to calibrate χ, and a number-average polymerization of $N = 50$. The polydispersity increases the periodicity of the lamellar phase,[46,50,51] and so the simulation boxes are enlarged so that they continue to contain approximately three periods. The simulation results for parallel-tempering runs starting from disorder and order are shown in Figure 6, for the different lattice site occupancies, Z.

The ODTs for monodisperse and polydisperse melts are extracted from Figures 4 and 6, respectively, and plotted in Figure 7 as a function of Đ. The plot also includes the ODT from SCFT,[50] corresponding to infinite $\bar{N}$. The mean-field ODT is reasonably linear even up to Đ $\lesssim 1.4$, which justifies our approximation in eq 3. Therefore, the simulation ODTs in Figure 7 are fit to straight lines, from which the coefficient γ_1 is obtained for four different $\bar{N}$ values. Figure 8 shows that the results are well described by the two-parameter fit

$$\gamma_1 \approx -0.77 + 17.5\bar{N}^{-0.49} \tag{11}$$

where the $\bar{N} \to \infty$ limit is constrained to match the SCFT prediction. Interestingly, the correction switches sign around $\bar{N} \approx 600$.

The second correction in eq 3 requires analogous simulations for monodisperse diblocks of asymmetric composition. Fortunately, Ghashimakbari and Morse[29] have recently published such simulations for $\bar{N} = 480$ and 1920. Figure 9 plots their ODTs together with the SCFT

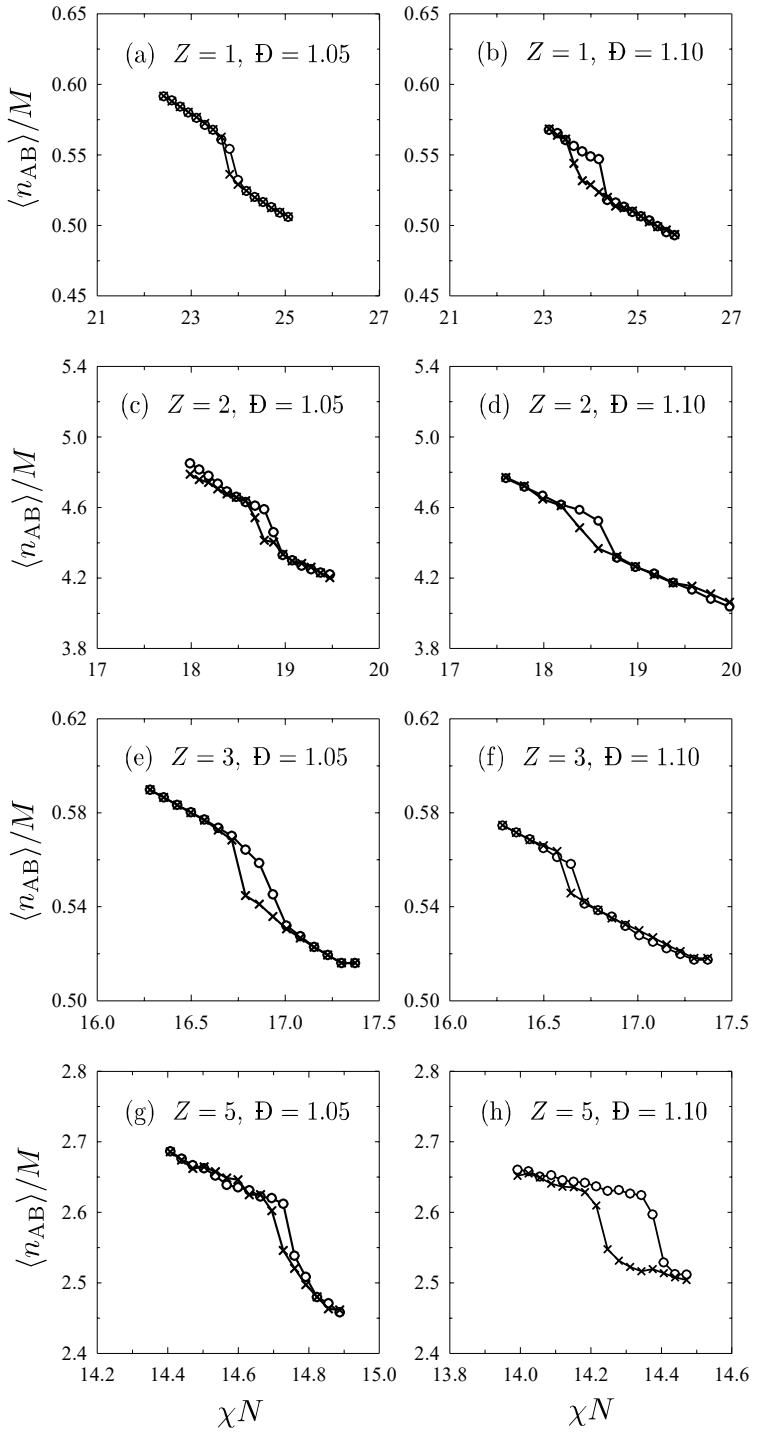


Figure 6: Analogous plots to those of Figure 4, but for polydisperse melts with a number-average polymerization of $N = 50$.

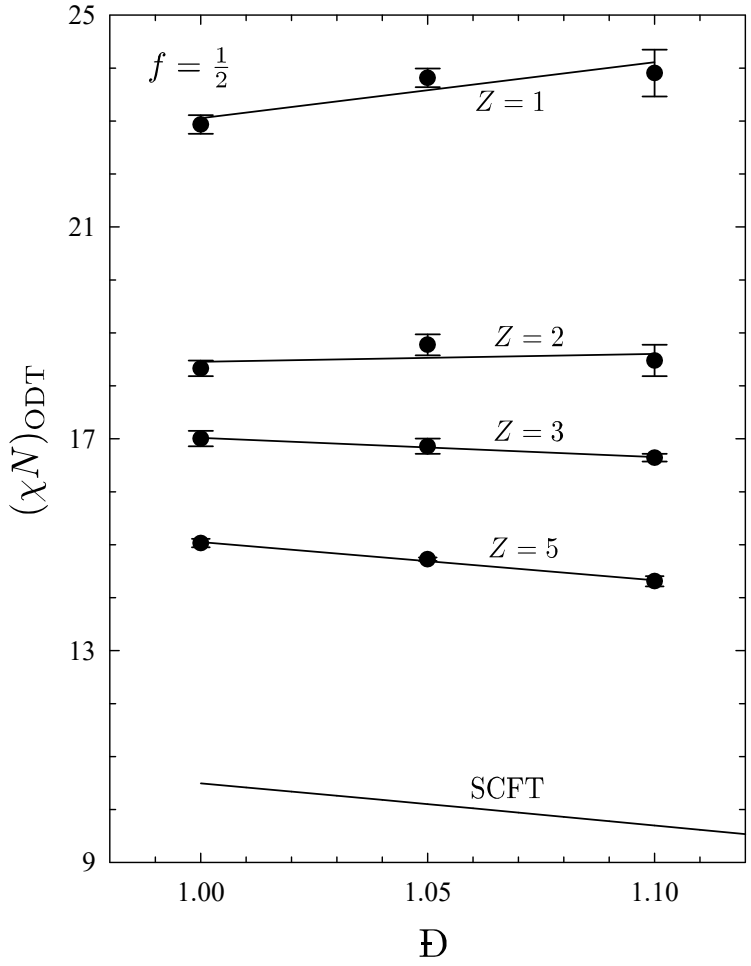


Figure 7: ODTs for monodisperse and polydisperse diblocks obtained from Figures 4 and 6, respectively. Linear fits are shown with solid lines. The bottom curve shows the mean-field ODT from SCFT.

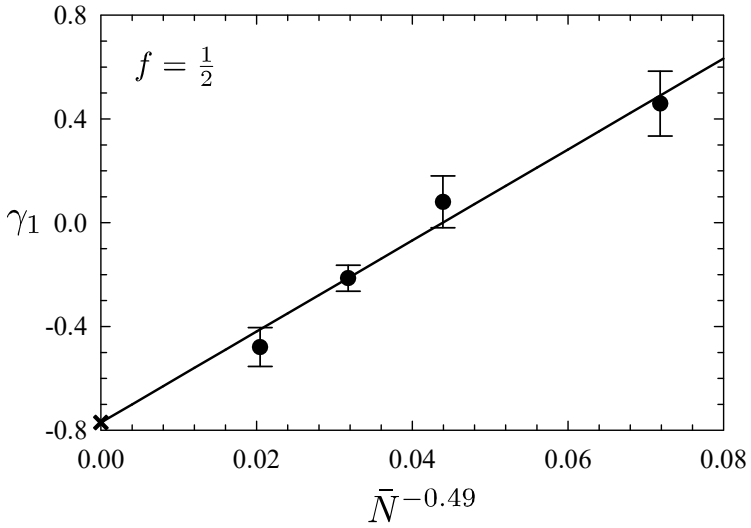


Figure 8: Coefficient for the polydispersity correction, γ_1, in eq 3 obtained from Figure 7. The line shows the empirical fit in eq 11, which was constrained to match the SCFT prediction denoted by a cross.

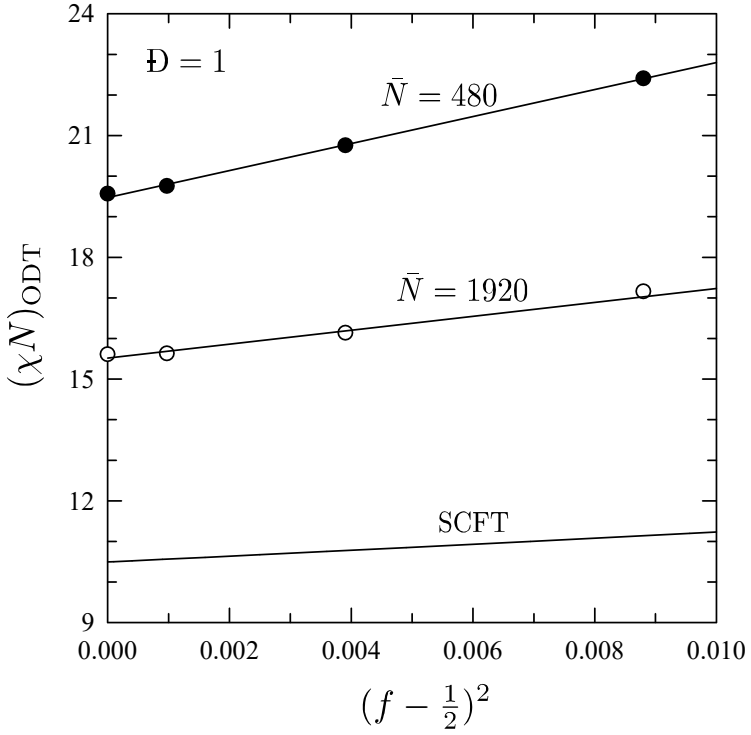


Figure 9: ODTs for compositionally-asymmetric monodisperse diblocks obtained from ref 29. Linear fits are shown with solid lines. The bottom curve shows the mean-field ODT from SCFT.

prediction,[3] corresponding to $\bar{N} \to \infty$. The linearity of the SCFT curve suggests that the parabolic approximation in eq 3 is reasonably accurate over most of the lamellar phase. Therefore, we again fit the simulation ODTs in Figure 9 to straight lines, which gives $\gamma_2 = 17$ and 11 for $\bar{N} = 480$ and 1920, respectively. These results are fit to

$$\gamma_2 \approx 6.7 + 500\bar{N}^{-0.63} \tag{12}$$

where again the first coefficient is obtained from SCFT.

Fits to Experiment

Since experimentalists routinely report the composition, f, and polydispersity, Đ, of their molecules, we are able to reanalyze previous calibrations based on ODT measurements, $T_{\rm ODT}$, of symmetric diblocks with different number-average molecular weights, M_n. For each diblock, we evaluate N from M_n, which requires the mass density, $\rho_{m,\gamma}$, for each component γ. To evaluate $\bar{N} = a^6\rho_0^2 N$, we require a_γ for each component, which is calculated from the ratio R_0^2/M_n, where R_0 is the natural end-to-end length of a homopolymer of molecular weight M_n. For simplicity, we use literature values of $\rho_{m,\gamma}$ and R_0^2/M_n at a fixed temperature of $T = 140°$C.[52–54] Once the required parameters are determined, the diblock ODTs are fit to a prediction of $(\chi N)_{\rm ODT}$, assuming the standard functional form

$$\chi(T) = \frac{A}{T} + B \tag{13}$$

where A and B are fitting parameters and T is expressed in terms of absolute temperature. To illustrate the dependence on the choice of $(\chi N)_{\rm ODT}$, fits are performed for four different predictions: mean-field theory, Fredrickson-Helfand theory, eq 1, and eqs 2-3.

Figure 10 shows the four estimates of $\chi(T)$ obtained from poly(ethylene)-poly(ethylenepropylene) diblock polymers,[40] which have exceptionally large invariant polymerization indices of $\bar{N} \approx$

2.5×10^4. Because of the large $\bar{N}$, the estimate based on the simple mean-field prediction, $(\chi N)_{\mathrm{ODT}} = 10.495$, is reasonably accurate. Nevertheless, the Fredrickson-Helfand prediction provides a $\sim 5\%$ improvement upwards and the ROL-based prediction in eq 1 increases this by another $\sim 2\%$. The correction for polydispersity decreases the estimate for $\chi(T)$ given that $\bar{N} \gtrsim 600$, while the correction for compositional asymmetry increases the estimate. In this case, the correction for polydispersity dominates, and the net consequence is a $\sim 2\%$ reduction in χ.

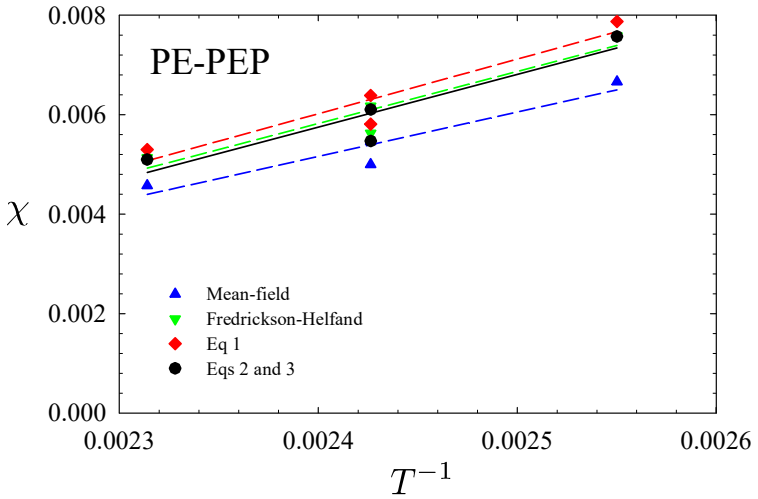


Figure 10: Flory-Huggins χ parameter for PE-PEP, obtained by fitting to different predictions of $(\chi N)_{\mathrm{ODT}}$.

Figure 11 provides analogous results for poly(DL-lactide)-poly(isoprene) diblocks,[37] but this time for exceptionally small indices of $\bar{N} \approx 2.5 \times 10^2$. As such, fluctuation effects are considerable, and consequently the estimate of $\chi(T)$ based on the mean-field ODT is terribly inaccurate. Even the estimate based on the Fredrickson-Helfand ODT is far from accurate compared to the ROL-based prediction in eq 1. Given the small $\bar{N}$, the additional corrections due to polydispersity and compositional asymmetry both increase the estimate of $\chi(T)$, with the former being significantly more important in this instance.

Our Supplementary Information summarizes the experimental data and details the calculations used to generate Figures 10 and 11 for the PE-PEP and PLA-PI diblocks, respectively, as well as 17 other chemical pairs. Table 2 lists the fitting parameters for the most accurate

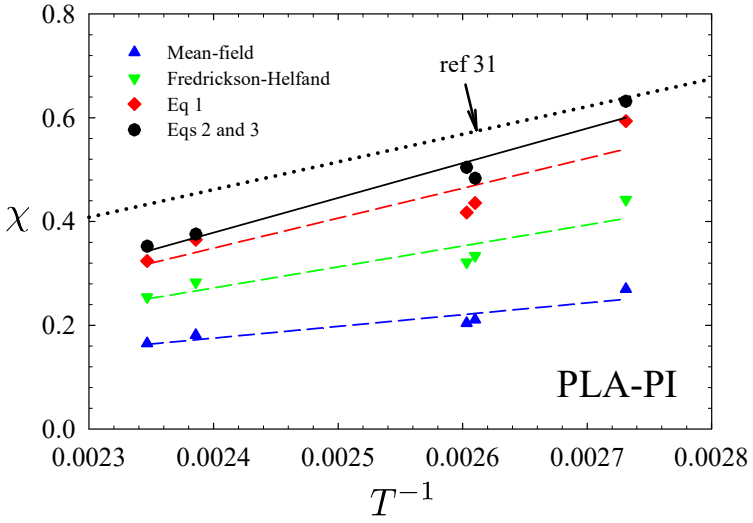


Figure 11: Analogous plot to that of Figure 10, but for PLA-PI. The dotted line denotes a previous estimate based on a Morse-type calibration modified for polydispersity.[31]

Table 2: Interaction parameters, $\chi(T) = A/T + B$, for different chemical pairs, obtained by fitting previously published ODT measurements to eqs 2-3. The calculations assume that T is expressed in units of Kelvin and that segments are defined based on a reference volume of $\rho_0^{-1} = 118$ Å^3.

chemical pair	ref	A	$B \times 10^3$
PE-PEP	40	10.60	-19.68
PEP-PEE	40	5.40	0.72
PCHE-PEE	33	21.6	-19.2
PE-PEE	40	10.5	6.0
PCHE-PEP	33	33.7	-22.2
PEE-PDMS	34	86.0	-151.3
PCHE-PE	33	62.1	-60.0
PS-PI	9,13,55	79.3	-131.5
PLA-PS	36	125	-163
PE-PDMS	34	123	-97
PEP-PDMS	34	68	-2
PI-PEO	13,55	255	-314
PCHE-PMMA	38	543	-707
PLA-PEE	39	647	-931
PE-PEO	34	722	-1275
PLA-PEP	35	875	-1393
PLA-PI	37	669	-1227
PEO-PEP	34	416	-540
PEO-PEE	34	475	-649

ROL-based prediction of $(\chi N)_{\mathrm{ODT}}$ using eqs 2-3. Note that these estimates of $\chi(T)$ are based on a segment volume of $\rho_0^{-1} = 118\text{Å}^3$. One can readily convert to other choices of the reference volume using the fact that $\chi \propto \rho_0^{-1}$.

Discussion

Our calibration of $\chi(T)$ based on eqs 2-3 is just about as easy to implement as the common practice of using $(\chi N)_{\mathrm{ODT}} = 10.495$, but far more accurate. The greatest improvement comes from replacing the mean-field prediction by the accurate one in eq 1. This is, in principle, equivalent to the Morse calibration, where experimental measurements of $S(q^*)$ are fit to ROL predictions, but avoids the need for measuring absolute scattering intensity. Furthermore, our approach includes a correction factor, Γ, to account for the small degrees of polydispersity and compositional asymmetry that always occur in real polymers.

Arora et al.[13,56] previously compared the Morse calibration to that of fitting ODTs to eq 1 for PS-PI and PS-PEO diblocks, and found reasonable agreement even without accounting for polydispersity or compositional asymmetry. In Figure 11, the dotted line shows the Morse-type calibration from ref 31 for PLA-PI diblocks, obtained by fitting $S(q^*)$ from a single diblock to simulations with an equivalent polydispersity of $Đ = 1.10$. This still neglects the compositional asymmetry of $f = 0.51$, but this level of asymmetry is insufficient to explain the difference with our new calibration method. Interestingly though, there is excellent agreement for the data point at $T^{-1} = 0.00273$, which in fact corresponds to the diblock used in the Morse-type calibration. The fact that the Morse calibration uses just a single molecule implies that it is more prone to experimental errors compared to the ODT-based calibration, which in this case combines results from five different molecules.

The correction factor, Γ, in eq 3 will, in principle, depend on the detailed shape of the polydispersity distribution,[57,58] but this dependence will be negligible for values of $Đ$ close to one.[50] It will also depend on the difference in A- and B-block polydispersities, which has

not been accounted for. However, the effect due to polydispersity is already small and thus the added correction will be tiny, since it will be proportional to $(Đ_A - Đ_B)^2$ due to the A-B symmetry about which we are expanding.

Another correction that could be incorporated into Γ is that of conformational asymmetry, $a_A \neq a_B$. Our lattice model could easily handle this asymmetry by introducing a small bending penalty for one of the components, but the Morse calibration of the revised model would not be so straightforward. It would require new ROL calculations of $S(q^*)$ for conformational asymmetry. Furthermore, the fit to $S(q^*)$ would be less constrained, because

$$\chi(\alpha) = c_0 + c_1\alpha + c_2\alpha^2 + c_3\alpha^3 + \cdots \tag{14}$$

would need to include a zeroth-order entropic contribution, c_0, and the first-order coefficient would no longer be given by $c_1 = z_\infty$. Although conformational asymmetry has a significant effect on order-order transitions, its effect on the ODT is relatively small, certainly in mean-field theory.[59] Therefore, we leave this small refinement for future consideration.

Now that we have an improved theoretical prediction for $(\chi N)_{ODT}$, the accuracy of $\chi(T)$ will undoubtedly be limited by the experiments.[13] The issue is the experimental uncertainties in molecular weights, densities, segment lengths, polydispersities, and ODT measurements, which have generally been ignored in the past. Given the analytical expressions in eqs 1, 2, 3, 11, and 12 for $(\chi N)_{ODT}$, researchers now have the opportunity to assess the inaccuracy in $\chi(T)$ by performing a rigorous error analysis. An advantage of the present approach is that it uses the ODTs from multiple molecules, and thus random errors can be averaged out by using more molecules. The fact that the ODT has a strong dependence on $\chi(T)$ will also help, in contrast to fits based on other quantities such as interfacial width,[10,22] interfacial tension,[10] or domain size.[10,36]

As mentioned in the Introduction, the multitude of inaccurate calibration methods has lead to the belief that $\chi(T)$ has significant dependencies on parameters other than tempera-

ture, such as molecular weight, polydispersity, composition, and even molecular architecture. Hopefully, these dependences are not real, or at least not significant. If χ did, indeed, depend on all the details of the system, then theory would lose its ability to make meaningful quantitative predictions. This concern was raised by Maurer et al.[11] when they found large differences in the values of $\chi(T)$ derived from diblock polymer melts as opposed to binary homopolymer blends. However, with all the experimental uncertainties involved, it is virtually impossible to ascertain the reason for this discrepancy. Simulations, arguably, offer a more reliable test of universality, simply because they are free of such uncertainties. So far, simulations have found excellent agreement between diblock melts and homopolymer blends.[43,60]

Hopefully, by using improved estimates of χ, the experimental discrepancies between different methods and different systems will largely vanish. Still, some dependencies are likely to remain. Simulations may suggest otherwise, but they typically involve structurally equivalent species (e.g., spherical beads of the same diameter and springs with the same bonding potential), where diblocks transform into homopolymers in the athermal limit (i.e., $\alpha \to 0$). This symmetry is responsible for reducing the general expansion for $\chi(\alpha)$ in eq 14 to that of eq 10. Without the symmetry, a diblock polymer still possesses distinct blocks in the athermal limit, each with different values of z_∞. Müller[61] has investigated entropic contributions resulting from differences in the monomer shape and chain stiffness, but it would be useful to examine these further. The packing of structurally distinct polymers will undoubtedly depend on composition, but hopefully these dependencies will prove to be relatively minor for most experimental systems.

It is important to remember that the universality hypothesis relies on high molecular weights, and thus it will gradually break down for short molecules. The value of N at which this happens remains to be determined, and it will certainly be system dependent. For instance, chain stiffness, long-range interactions, and anisotropic interactions will increase the required threshold for universality. This is as true for simulation models as for experimental

systems. In fact, our choice of $N = 50$ was motivated by evidence that deviations from universality appear to emerge for $N \lesssim 30$.[43] For systems that do not adhere to universality, it will be necessary to go beyond the standard Gaussian chain model and the assumption that molecular interactions can be accounted for by a single χ parameter. For example, we may need to consider liquid-crystalline interactions, the finite range of the interactions, and/or separate interactions for chain-end groups.[55,62]

Summary

We have improved upon one of the common methods of estimating the Flory-Huggins χ parameter, whereby the order-disorder transitions (ODTs) of symmetric diblock polymer melts are fit to mean-field theory. The original method benefits from the fact that T_{ODT} can be accurately measured and the fact that it has a strong dependence on χ. However, the method suffers from the serious drawback that the mean-field prediction, $(\chi N)_{\mathrm{ODT}} = 10.495$, is highly inaccurate due to fluctuations. Fortunately, this shortcoming is easily remedied by switching to the accurate expression in eq 1. Three separate comparisons have now shown that this produces comparable predictions to the more complicated Morse calibration,[30,31,63] where the peak of the disordered-state structure function, $S(q^*)$, is fit to renormalized one-loop (ROL) calculations.

The accuracy of our new method is further improved with the correction factor, Γ, in eq 3, which accounts for small deviations from ideal molecules of $Đ = 1$ and $f = \frac{1}{2}$. The first correction (γ_1 in eq 11) was obtained by calibrating a multiple-occupancy lattice model and using it to evaluate the shift in $(\chi N)_{\mathrm{ODT}}$ due to small degrees of polydispersity typical of experiment for a wide range of invariant polymerization indices, $\bar{N}$. The second correction for compositional asymmetry (γ_2 in eq 12) was extracted from previous simulations by Ghasimakbari and Morse.[29]

The resulting calibration method was then applied to 19 different chemical pairs. The

switch from $(\chi N)_{\mathrm{ODT}} = 10.495$ to eq 1 can increase the predicted value of χ by more than a factor of two, particularly for lower molecular-weight molecules. The correction for polydispersity is smaller but still significant, reducing the predicted χ for large molecules and increasing it for small molecules. The final correction for compositional asymmetry causes a slight increase in χ for all values of $\bar{N}$.

Other potential refinements to our method could account for distinct polydispersities in each block, $Đ_{\mathrm{A}} \neq Đ_{\mathrm{B}}$, and for conformational asymmetry, $a_{\mathrm{A}} \neq a_{\mathrm{B}}$. The first would be relatively straightforward to evaluate, but is likely too small to justify the experimental effort required to measure the individual polydispersities. The second is more challenging to evaluate due to difficulties in calibrating models with structurally different blocks, but its effect is nevertheless expected to be relatively minor.

Now that the estimate of $(\chi N)_{\mathrm{ODT}}$ has been improved, the next challenge is to reduce experimental uncertainties. More precise synthesis and characterization measurements will naturally help, as will using a greater number of molecules in the fits to reduce random errors. The analytical expression for $(\chi N)_{\mathrm{ODT}}$ will make it possible to perform thorough error analyses in order to assess the accuracy of $\chi(T)$. The increased rigor will undoubtedly lead to better quantitative agreement between theory and experiment, which in turn will help researchers investigate the finer details of block polymer behavior, such as for example chain-end effects.[55,62]

Supporting Information

Details of the $\chi(T)$ calibrations for the 19 chemical pairs in Table 2.

ORCID

J. D. Willis: 0000-0003-1441-9403

T. M. Beardsley: 0000-0002-6551-7866

M. W. Matsen: 0000-0003-2099-0892

Acknowledgments

This work was supported by NSERC of Canada, and computer resources were provided by Compute Canada.

References

(1) Glaser, J.; Qin, J.; Medapuram, P.; Müller, M.; Morse, D. C. Test of a Scaling Hypothesis for the Structure Factor of Disordered Diblock Copolymer Melts. *Soft Matter* **2012**, *8*, 11310.

(2) Matsen, M. W. The Standard Gaussian Model for Block Copolymer Melts. *J. Phys.: Condens. Matter* **2002**, *14*, R21–R47.

(3) Matsen, M. W.; Bates, F. S. Unifying Weak- and Strong-Segregation Block Copolymer Theories. *Macromolecules* **1996**, *29*, 1091–1098.

(4) Fredrickson, G. H. *The Equilibrium Theory of Inhomogeneous Polymers*; Oxford University Press: New York, 2006.

(5) Matsen, M. W. In *Soft Matter: Polymer Melts and Mixtures*; Gompper, G., Schick, M., Eds.; Wiley-VCH: Weinheim, Germany, 2006.

(6) Matsen, M. W. Field Theoretic Approach for Block Polymer Melts: SCFT and FTS. *J. Chem. Phys.* **2020**, *152*, 110901.

(7) Fredrickson, G. H.; Helfand, E. Fluctuation Effects in the Theory of Microphase Separation in Block Copolymers. *J. Chem. Phys.* **1987**, *87*, 697–705.

(8) Russell, T. P.; Hjelm, Jr., R. P.; Seeger, P. A. Temperature Dependence of the Interaction Parameter of Polystyrene and Poly(methyl methacrylate). *Macromolecules* **1990**, *23*, 890–893.

(9) Lin, C.; Jonnalagadda, S.; Kesani, P.; Dai, H.; Balsara, N.; Effect of Molecular Structure on the Thermodynamics of Block Copolymer Melts. *Macromolecules* **1994**, *27*, 7769–7780.

(10) Clarke, C. J.; Eisenberg, A.; La Scala, J.; Rafailovich, M. H.; Sokolov, J.; Li, Z.; Qu, S.; Nguyen, D.; Schwarz, S. A.; Strzhemechny, Y.; Sauer, B. B. Measurements of the Flory–Huggins Interaction Parameter for Polystyrene–Poly(4-vinylpyridine) Blends. *Macromolecules* **1997**, *30*, 4184–4188.

(11) Maurer, W. W.; Bates, F. S.; Lodge, T. P.; Almdal, K.; Mortensen, K.; Fredrickson, G. H. Can a Single Function for χ Account for Block Copolymer and Homopolymer Blend Phase Behavior? *J. Chem. Phys.* **1998**, *108*, 2989–3000.

(12) Miqueland-Garnier, G.; Roland, S. Beware of the Flory Parameter to Characterize Polymer-Polymer Interactions: A Critical Reexamination of the Experimental Literature. *Euro. Polym. J.* **2016**, *84*, 111–124.

(13) Arora, A.; Pillai, N.; Bates, F. S.; Dorfman, K. D. Predicting the Phase Behavior of ABAC Tetrablock Terpolymers: Sensitivity to Flory–Huggins Interaction Parameters. *Polymer* **2018**, *154*, 305–314.

(14) Owens, J. N.; Gancarz, I. S.; Koberstein, J. T.; Russell, T. P. Investigation of the Microphase Separation Transition in Low-Molecular-Weight Diblock Copolymers. *Macromolecules* **1989**, *22*, 3380–3387.

(15) Koch, T.; Strobl, G. R. Concentration Dependence of the Flory–Huggins Interaction Parameter of a Polymer Blend as Determined by Smal–Angle X–Ray Scattering Experiments. *J. Polym. Sci., Part B* **1990**, *28*, 343–353.

(16) Dai, K. H.; Kramer, E. J. Determining the Temperature–Dependent Flory Interaction Parameter for Strongly Immiscible Polymers from Block Copolymer Segregation Measurements. *Polymer* **1994**, *35*, 157–161.

(17) Zha, W.; Han, C. D.; Lee, D. H.; Han, S. H.; Kim, J. K.; Kang, J. H; Park, C. Origin of the Difference in Order–Disorder Transition Temperature between Polystyrene-block-poly(2-vinylpyridine) and Polystyrene-block-poly(4-vinylpyridine) Copolymers. *Macromolecules* **2007**, *40*, 2109–2119.

(18) Han, S. H.; Kim, J. K. Temperature–Dependent Interaction Parameters of Poly(methyl methacrylate)/Poly(2-vinyl pyridine) and Poly(methyl methacrylate)/Poly(4-vinyl pyridine) Pairs. *React. Funct. Polym.* **2009**, *69*, 493–497.

(19) Sweat, D. P.; Kim, M.; Larson, S. R.; Choi, J. W.; Choo, Y.; Osuji, C. O.; Gopalan, P. Rational Design of a Block Copolymer with a High Interaction Parameter. *Macromolecules* **2014**, *47*, 6687–6696.

(20) Hofman, A. H.; Alberda van Ekenstein, G. O. R.; Woortman, A. J. J.; ten Brinke, G.; Loos, K. Poly(4-vinylpyridine)-block-Poly(N-acryloylpiperidine) Diblock Copolymers: Synthesis, Self–Assembly and Interaction. *Polym. Chem.* **2015**, *6*, 7015–7026.

(21) Zhou, S. X.; Janes, D. W.; Kim, C. B.; Willson, C. G.; Ellison, C. J. Designing Intrablock Attractions to Increase the Chi Parameter of a Symmetric Diblock Copolymer. *Macromolecules* **2016**, *49*, 8332–8340.

(22) Burns, A. B.; Christie, D.; Mulhearn, W. D.; Register, R. A. Estimating the Segregation Strength of Microphase-Separated Diblock Copolymers from the Interfacial Width. *J. Polym. Sci., Part B* **2019**, *57*, 932–940.

(23) Glaser, J.; Medapuram, P.; Morse, D. C. Collective and Single-Chain Correlations in Disordered Melts of Symmetric Diblock Copolymers: Quantitative Comparison of Simulations and Theory. *Macromolecules* **2014**, *47*, 851-869.

(24) Grzywacz, P.; Qin, J.; Morse, D. C. Renormalization of the One-Loop Theory of Fluctuations in Polymer Blends and Diblock Copolymer Melts. *Phys. Rev. E* **2007**, *76*, 061802.

(25) Qin, J.; Grzywacs, P.; Morse, D. C. Renormalized One-Loop Theory of Correlations in Disordered Diblock Copolymers. *J. Chem. Phys.* **2011**, *135*, 084902.

(26) Glaser, J.; Medapuram, P.; Beardsley, T. M.; Matsen, M. W.; Morse, D. C. Universality of Block Copolymer Melts. *Phys. Rev. Lett.* **2014**, *113*, 068302.

(27) Medapuram, P.; Glaser, J.; Morse, D. C. Universal Phenomenology of Symmetric Diblock Copolymers near the Order–Disorder Transition. *Macromolecules* **2015**, *48*, 819–839.

(28) Ghasimakbari, T.; Morse, D. C. Correlations in Disordered Melts of Asymmetric Diblock Copolymers. *Macromolecules* **2018**, *51*, 2335–2348.

(29) Ghasimakbari, T.; Morse, D. C. Order-Disorder Transitions and Free Energies in Asymmetric Diblock Copolymers. *Macromolecules* **2018**, *53*, 7399–7409.

(30) Gillard, T. M.; Medapuram, P.; Morse, D. C.; Bates, F. S. Fluctuations, Phase Transitions, and Latent Heat in Short Diblock Copolymers: Comparison of Experiment, Simulation, and Theory. *Macromolecules* **2015**, *48*, 2801–2811.

(31) Beardsley, T. M.; Matsen, M. W. Universality between Experiment and Simulation of a Diblock Copolymer Melt. *Phys. Rev. Lett.* **2016**, *117*, 217801.

(32) Bates, F. S.; Schultz, M. F.; Rosedale, J. H.; Almdal, K. Correlation of Binary Polyolefin Phase Behavior with Statistical Segment Length Asymmetry. *Macromolecules* **1992**, *25*, 5547–5550.

(33) Cochran, E. W.; Bates, F. S. Thermodynamic Behavior of Poly(cyclohexylethylene) in Polyolefin Diblock Copolymers. *Macromolecules* **2002**, *35*, 7368–7374.

(34) Almdal K.; Hillmyer, M. A.; Bates, F. S. Influence of Conformational Asymmetry on Polymer-Polymer Interactions: An Entropic or Enthalpic Effect? *Macromolecules* **2002**, *35*, 7685–7691.

(35) Schmidt, S. C.; Hillmyer, M. A. Morphological Behavior of Model Poly(ethylene-alt-propylene)-b-Polylactide Diblock Copolymers. *J. Polym. Sci., Part B* **2002**, *40*, 2364–2376.

(36) Zalusky, A. S.; Olayo-Valles, R.; Wolf, J. H.; Hillmyer, M. A. Ordered Nanoporous Polymers from Polystyrene-Polylactide Block Copolymers. *J. Am. Chem. Soc.* **2002**, *124*, 12761–12773.

(37) Lee, S.; Gillard, T. M.; Bates, F. S. Fluctuations, Order, and Disorder in Short Diblock Copolymers. *AIChE J.* **2013**, *59*, 3502–3513.

(38) Kennemur, J. G.; Yao, L.; Bates, F. S.; Hillmyer, M. A. Sub-5 nm Domains in Ordered Poly(cyclohexylethylene)-block-Poly(methyl methacrylate) Block Polymers for Lithography. *Macromolecules* **2014**, *47*, 1411–1418.

(39) Schulze, M. W.; Lewis III, R. M.; Lettow, J. H.; Hickey, R. J.; Gillard, T. M.; Hillmyer, M. A.; Bates, F. S. Conformational Asymmetry and Quasicrystal Approximants in Linear Diblock Copolymers. *Phys. Rev. Lett.* **2017**, *118*, 207801.

(40) Rosedale, J. H.; Bates, F. S.; Almdal, K.; Mortensen, K.; Wignall, G. D. Order and Disorder in Symmetric Diblock Copolymer Melts. *Macromolecules* **1995**, *28*, 1429–1443.

(41) Mulhearn, W. D.; Register, R. A. Melt Miscibility in Diblock Copolymers Containing Polyethylene and Substituted Hydrogenated Polynorbornenes. *Macromolecules* **2017**, *50*, 5830–5838.

(42) Jun, T.; Lee, Y.; Jo, S.; Ryu, C. Y.; Ryu, D. Y. Composition Fluctuation Inhomogeneity of Symmetric Diblock Copolymers: χN Effects at Order-to-Disorder Transition. *Macromolecules* **2018**, *51*, 282–288.

(43) Willis, J. D.; Beardsley, T. M.; Matsen, M. W. Calibration of a Lattice Model for High-Molecular-Weight Block Copolymer Melts. *J. Chem. Phys.* **2019**, *150*, 204906.

(44) Schulz, G. V. The Kinetics of Chain Polymerisation V. The influence of Various Types of Reactions on the Poly–molecularity *Z. Phys. Chem. (Munich)* **1939**, *B43*, 25–46.

(45) Zimm, B. H. Apparatus and Methods for Measurement and Interpretation of the Angular Variation of Light Scattering; Preliminary Results on Polystyrene Solutions. *J. Chem. Phys.* **1948**, *16*, 1099–1116.

(46) Beardsley, T. M.; Matsen, M. W. Effects of Polydispersity on the Order–Disorder Transition of Diblock Copolymer Melts. *Eur. Phys. J. E* **2008**, *27*, 323–333.

(47) Morse, D. C.; Chung, J. K. On the Chain Length Dependence of Local Correlations in Polymer Melts and a Perturbation Theory of Symmetric Polymer Blends. *J. Chem. Phys.* **2009**, *130*, 224901.

(48) Beardsley, T. M.; Matsen, M. W. Monte Carlo Phase Diagram for Diblock Copolymer Melts. *Eur. Phys. J. E* **2010**, *32*, 255–264.

(49) Arora, A.; Morse, D. C.; Bates, F. S.; Dorfman, K. D. Commensurability and Finite Size Effects in Lattice Simulations of Diblock Copolymers. *Soft Matter* **2015**, *11*, 4862–4867.

(50) Cooke, D. M.; Shi, A.-C. Effects of Polydispersity on Phase Behavior of Diblock Copolymers. *Macromolecules* **2006**, *39*, 6661–6671.

(51) Matsen, M. W. Effects of Large Degrees of Polydispersity on Strongly-Segregated Block Copolymers. *Eur. Phys. J. E* **2006**, *21*, 199–207.

(52) Fetters; L. J.; Lohse, D. J.; Richter, D.; Witten, T. A.; Zirkel A. Connection between Polymer Molecular Weight, Density, Chain Dimensions, and Melt Viscoelastic Properties. *Macromolecules* **1994**, *27*, 4639–4647.

(53) Anderson, K. S.; Hillmyer, M. A. Melt Chain Dimensions of Polylactide. *Macromolecules* **2004**, *37*, 1857–1862.

(54) Henton, D. E.; Gruber, P.; Lunt, J.; Randall, J. In *Natural Fibers, Biopolymers, and Biocomposites*, Mohanty, A. K., Misra, M., Drzal, L. T., Eds.; CRC Press: New York, 2005.

(55) Frielinghaus, H.; Hermsdorf, N.; Sigel, R.; Almdal, K.; Mortensen, K.; Hamley, I. W .; Messe, L.; Corvazier, L.; Ryan, A. J.; van Dusschoten, D.; Wilhelm, M.; Foudas, G.; Fytas, G. Blends of AB/BC Diblock Copolymers with a Large Interaction Parameter χ. *Macromolecules* **2001**, *34*, 4907–4916.

(56) Arora, A.; Pillai, N.; Bates, F. S.; Dorfman, K. D. Erratum to "Predicting the Phase Behavior of ABAC Tetrablock Terpolymers: Sensitivity to Flory–Huggins Interaction Parameters" [Polymer, 154 (2018), 305–314]. *Polymer* **2020**, *210*, 123038.

(57) Lynd, N. A.; Hillmyer, M. A.; Matsen, M. W. Theory of Polydisperse Block Copolymer Melts: Beyond the Schulz-Zimm Distribution. *Macromolecules* **2008**, *41*, 4531–4533.

(58) Listak, J.; Jakubowski, W.; Mueller, L.; Plichta, A.; Matyjaszewski, K.; Bockstaller, M. R. Effect of Symmetry of Molecular Weight Distribution in Block Copolymers on Formation of "Metastable" Morphologies. *Macromolecules* **2008**, *41*, 5919–5927.

(59) Matsen, M. W.; Bates, F. S. Conformationally Asymmetric Diblock Copolymers. *J. Polym. Sci., Part B* **1997**, *35*, 945–952.

(60) Beardsley, T. M.; Matsen, M. W. Fluctuation Correction for the Critical Transition of Symmetric Homopolymer Blends. *J. Chem. Phys.* **2017**, *147*, 044905.

(61) Müller, M. Effects of Structural Disparities in Polymer Blends: A Monte-Carlo Investigation. *Macromolecules* **1995**, *28*, 6556–6564.

(62) Kim, J.; Jung, H. Y.; Park, M. J. End-Group Chemistry and Junction Chemistry in Polymer Science: Past, Present, and Future. *Macromolecules* **2020**, *53*, 746–763.

(63) Medapuram, P. Investigation of Universal Behavior in Symmetric Diblock Copolymer Melts, Ph. D. thesis, University of Minnesota, 2015.